NUMERICAL MODELS OF WASTE GLASS MELTERS
PART I – LUMPED PARAMETER ANALYSES OF DWPF

H. N. Guerrero and D. F. Bickford
Westinghouse Savannah River Co.
Aiken, SC 29808

ABSTRACT

Defense Waste Processing Facility melter production data from three waste batches were analyzed using a lumped parameter approach which separates effects of melter feed, heater temperature, and power on melt rate under various modes of operation. A detailed distribution of power inputs and heat consumption pathways, as provided by the lumped parameter model, evaluated possible causes of melt rate reduction and other operational data. Theoretical aspects of the steady state analysis, as well as transient analysis, are presented.The lumped model complements the more detailed multi-dimensional computational models by providing boundary conditions for such models, and is the only practical way of predicting transients.

INTRODUCTION

The Department of Energy's Defense Waste Processing Facility (DWPF) melter has operated for six years at varying rates. An examination of the power, materials flow and thermal data from radioactive operations was conducted to provide trend analyses and isolate sources of variation. Actual DWPF production data was evaluated using a lumped parameter approach which separates effects of melter feed, heater temperature, and power on melt rate under various modes of operation. This model can be used to:

- Facilitate the analyses of existing melter problems from a thermal perspective to determine possible improvements.
- Provide a rapid, disciplined way of evaluating relative effects of proposed methods of increasing melt rate and other changes to melter operation.
- Isolate and diagnose changes in the behavior of the melting process.
- Provide the boundary conditions such as shell heat losses, radiant heat fluxes to the cold cap and upper plenum for more detailed Computational Fluid Dynamics (CFD) analyses of the glass melt and cold cap.
- Obtain a transient analysis of melter operation and to acquire an insight into the physical mechanisms occurring during transients.

The lumped parameter method provides a steady state balance between melter power inputs and various power consumption pathways under continuous feeding/pouring or idling conditions. These various power losses include heat lost

through the melter shell, evaporation of feed water, heating of steam and in-leakage air, chemical reactions, and heating of glass. These are not constant and depend on melter operating conditions such as feed rate, solids ratio, feed batch and net pool circulation. Through this model, the separate effects of engineering and physical chemistry batch effects can be obtained for quick evaluation of their effects on melt rate. The thermal model also provides a framework where laboratory determination of batch effects, e.g., specific heat, viscosity, thermal conductivity, etc. can be varied and the relative melt rate effect predicted.

The lumped parameter model is inherently limited in that space variations in glass and cold cap temperatures and heat transfer coefficients for glass to cold cap convection are not accounted for. A 3-dimensional model using computational fluid dynamics is currently being developed which may in the future provide more accurate averaged parameters for this lumped parameter model.

OVERVIEW OF HISTORIC DWPF MELTER OPERATION

In this section, the performance of the DWPF Melter to date with three different feed compositions, termed macrobatches, is discussed. Daily DWPF Melter power data as a function of feed rate for the period, 11/97 to 2/98, representative of Macrobatch 1 feed, are summarized in Figure 1. The scatter of the total power data points around the linear trend-line is much tighter than for the corresponding data points for the electrode and dome heater powers. This suggests that it is the total power that is important and the trend-lines for the electrode power and dome heater power should also be linear. Using the equations for the trend-lines, it is apparent that the electrode power was initially high (173 kW) at zero feed and decreased slightly to 163 kW at 0.75 gpm. The dome heater power increased linearly from 103 kW at 0 gpm feed rate to 278 kW at 0.75 gpm. In DWPF operation, glass melt pool and dome heater temperature limits dictate the above power settings. These conditions resulted in a melt mass flux of 8 lbs/hr-ft^2 at the maximum feed of 0.75 gpm and 49% solids ratio. This was only 87 % of the value achieved in the SGM and IDMS runs. This may be attributable to scale-up effects; or, the current nitric acid flow sheet feed is slower melting than the formic acid flow sheet used for most of the pilot scale studies.

A similar set of daily power data for the period, 1/99 to 8/99, representing Macrobatch 2 runs, indicate that for Macrobatch 2, the melt rate decreased approximately 20% from that of Macrobatch 1. The maximum feed attained for Macrobatch 2 was 0.6 gpm, while the maximum for Macrobatch 1 was 0.75 gpm. The electrode power decreased for Macrobatch 2 (143 kW) relative to Macrobatch 1 (163 kW). For Macrobatch 3, the electrode power decreased to 101 kW, and the Macrobatch the melt rate decreased 27% from Macrobatch 1. The maximum feed for Macrobatch 3 was 0.5 gpm.

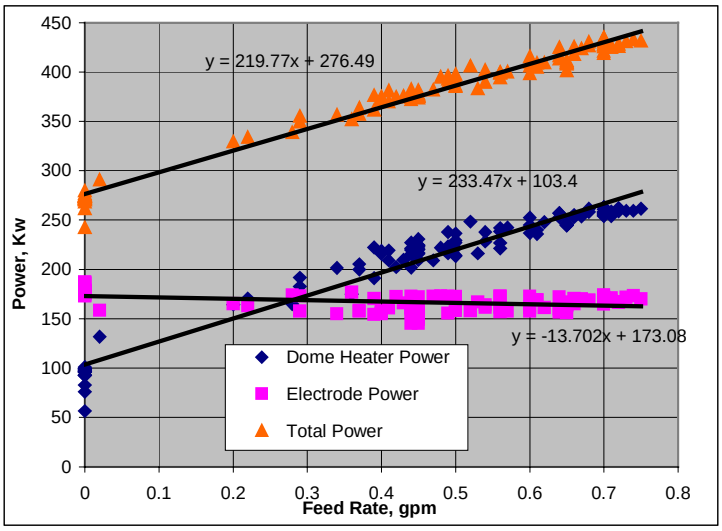

Figure 1 DWPF Melter Daily Averaged Power Data from 11/1/97 to 2/18/98 - Macrobatch 1

Under Macrobatch 1 and 2 conditions, the available power from the electrodes transferred to the cold cap directly from the melt pool or via the upper plenum was 90 kW and 68.5 kW, respectively. It was much less for Macrobatch 3, at 25.7 kW. The total power, or the sum of electrode and dome heater powers, for the three batches did not vary significantly since the energy to melt the glass was only a small fraction of the total energy input. The decrease in electrode power under feeding conditions may be attributed to the possible presence of a thermally resistant layer in the cold cap. The waste glass batches are known to have foaming characteristics. Under feeding conditions, this thermally resistant layer reduced convection heat transfer from the melt pool to the cold cap, thus decreasing electrode power requirement in order not to exceed the maximum glass temperature limit.

Under idling conditions, Macrobatch 3 electrode power decreased compared to Macrobatches 1 and 2, which were similar. The vapor space temperature also decreased by as much as 27C. Calculations show that the radiant heat from the glass surface decreased, as well as the effective cold cap surface temperature. This implies the presence of a thermally resistant layer, which may be due to persistent foam layer or accumulation of melt resistant layer.

DETAILED POWER INPUTS AND HEAT LOSS DISTRIBUTIONS

A detailed distribution of power consumption for Macrobatch 1 conditions may be determined by using the lumped parameter model to estimate component losses, which were not directly measured. Under feeding conditions of 2.65 lpm,

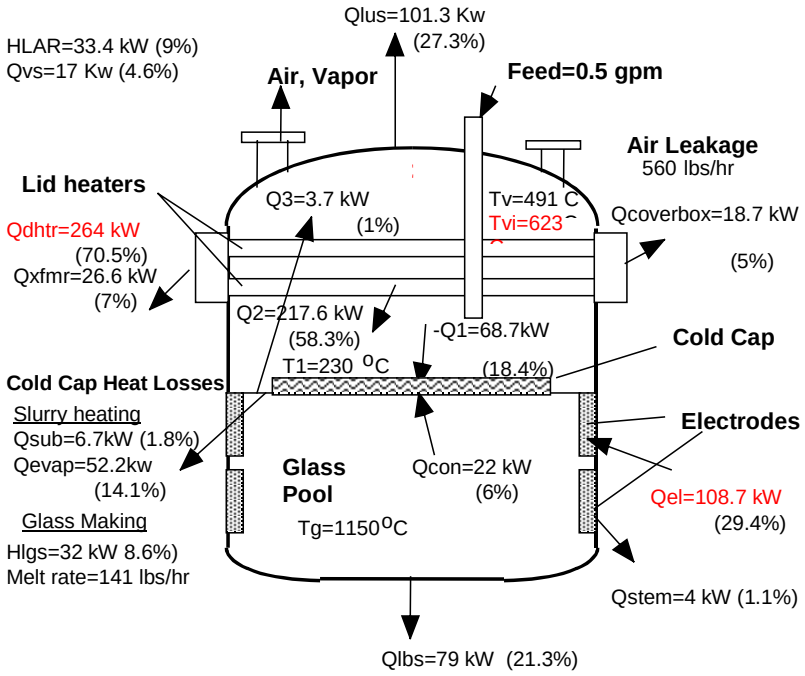

Figure 2 Distribution of Power Inputs and Power Consumption for Macrobatch 3

the electrode power required was 163 kW or 39.7% of the total power. The dome heater power was 266.8 kW. The energy required to eliminate subcooling and evaporate the water was19.7% (87 kW) of the total energy input and the actual amount of energy required to melt the glass was only 10.7% (47 kW). The shell heat losses amounted to about 41% of the total energy input and the energy lost by gas mass flux due to air in-leakage, steam and calcined gas was about 14.6%. The remainder was miscellaneous losses. The resulting melt mass flux was 39.7 Kgs/hr-m^2, which was 11 % less than assumed for the design conditions.

Power inputs and losses for Macrobatch 2 full feed conditions of 2.08 lpm were similar to Macrobatch 1. The melt rate was 30.7 Kgs/hr for a solids ratio of 49%, which was 30% less than the design value. The electrode power had dropped down to 138.4 kW (from 163 kW for Macrobatch 1) under full feed conditions. This suggests that something happened with the cold cap, perhaps significantly more foaming in Macrobatch 2, as compared to Macrobatch 1.

The power consumption for Macrobath 3 full feed conditions of 1.89 lpm, required an electrode power of 108.7 kW or 29.4% of the total power input. The dome heater power was 264 kW. The energy required to eliminate subcooling and evaporate the water was14.1% (52.2 kW) of the total energy input and the actual amount of energy required to melt the glass was only 8.6% (32 kW). The shell

heat losses amounted to about 48.6% of the total energy input and the energy lost by gas mass flux due to air in-leakage, steam and calcined gas was about 13.6%. The resulting melt mass flux was 27.9 Kg/hr-m^2, which was 37 % less than assumed for the design conditions.

With the lumped parameter model, it was possible to estimate the amount of heat directly transferred to the cold cap from the melt pool, 22 kW, which was much lower than in Macrobatches 1 and 2. The radiant heat absorbed by the cold cap from the dome heaters and plenum walls was 68.7 kW. Through the radiant heat exchange method (to be discussed later), the surface temperature of the cold cap was estimated as 230^{o}C. The corresponding values for Macrobatch 2, which has close to the same feed rate are: 400^{o}C and 52.7 kW. The cold cap temperature is an effective temperature, which implies that a large proportion of the cold cap is covered with wet slurry. It is clear that a highly insulating cold cap layer reduced heat addition to the cold cap from the melt pool. To make up for this, the dome heater power had to be increased, 264 kW (up from 243 kW for Macrobatch 2 for close to the same feed rate). This required a low cold cap surface temperature of 230^{o}C.

Under idling conditions, the indicated vapor space temperature (Tvi) decreased to 800^{o}C (from 892^{o}C in Macrobatch 1 and 883^{o}C in Macrobatch 2). The vapor temperatures, corrected for radiation heating effect, were 730 ^{o}C, 730 ^{o}C, and 649 ^{o}C. Using the lumped model for idling conditions, the glass surface temperature and the radiant flux from the glass surface can be predicted, to be 747^{o}C and 25.7 kW, respectively. The corresponding values for Macrobatches 1 and 2 are 900^{o}C, 877^{o}C and 90 kW, 87 kW, respectively. This appears to confirm the premise that a thermally resistant upper glass layer has formed, e.g., spinels.

ANALYTICAL METHOD

This analysis uses a lumped parameter approach for simplicity and to provide an overall perspective of a very complex process. The averaged or lumped parameters of the model can come from more detailed 3-dimensional computational fluid dynamics models currently in progress, from experiments, or from DWPF data. First a steady state heat balance of the melter is calculated. This calculation borrows heavily from the 1988 analysis of Yoshioka, (Ref. 1) including property parameter relations. The BASIC program archived for this work did not seem to correspond to the logic presented in Reference 1, and running that program did not provide the same results as in the report. In that report, the vapor temperature was assumed known, 680^{o}C at design conditions, and the demanded (required) electrode power and dome heater powers were calculated. Due to high actual upper shell heat losses in the melter, the measured vapor temperatures are much lower, typically 493^{o}C (with radiation correction) at 0.7 gpm (Macrobatch 1). Consequently, the heat balance calculation was redone,

using most of the same equations in the Basic program. The present calculation however differs from 1 in that the radiation heat transfer in the melter upper plenum accounts for radiation exchange among all the surfaces in the upper plenum and includes the steam as participating media. The results of the steady state heat balance closely resemble the results of Ref. 1 if the same inputs are used. The present analysis however assumes the electrode power, dome heater power, and feed rate are known functions of time. Further, estimates of the shell heat losses based on actual DWPF Melter power data, which are almost twice as much as those in Ref. 1, are used. Then the glass, vapor space, and dome heater temperatures, and internal heat distributions are then calculated.

Steady state equations

By performing a heat balance on the cold cap, Equation 1below follows. Here, the sum of the convective heat from the glass pool, Qcon, and the net radiant heat absorbed by the cold cap, -Q1, is used to evaporate the feed water, melt the glass, and raise its temperature to the operating temperature.

$$Qcon-Q1= SFR*cpw*(100-25) + SFR*\Delta Hevap + MR*Hbatch \qquad [1]$$

Where,

$$Hbatch = \left(\int_{20^oC}^{1150^oC} c_p dT + \int_{20^oC}^{1150^oC} \Delta H_r dT \right) = cpg*(Tsoft-25) + \Delta Hmelting + cpg*(1150-554),$$

ΔHmelting is estimated to be 120 cal/gm for endothermic reaction heat and –80 cal/gm for exothermic reaction, which includes 20 cal/gm for silica melting. SFR is the water (or steam) feed rate. ΔHevap is the heat of evaporation of water, cpw and cpg are the specific heats of water and glass, respectively. The average value of cpg over the appropriate temperature range is used in *Hbatch*.

The vapor space, lid heater, and plenum wall temperatures and the wall heat loss, radiant heat absorbed by the cold cap, and lid heater power are calculated by radiant heat exchange equations of the form,

$$Q_k = A_k \sigma [T_k^4 - \sum_{i=1}^{N} F_{ik} \tau_{ik} T_i^4 - \varepsilon_v T_v^4] \qquad [2]$$

assuming all surfaces are black. Here, σ is the Stefan-Boltzman constant, A_k is the area of the surface k, Fικ is the view factor from surface *i* to surface *k*, τ_{ik} is the transmittance , and ε_v is the emissivity of the vapor. The sum of all surface radiant heats into the plenum goes into heating the steam. The radiant heat absorbed by the walls equals the sum of the heat lost through the walls and transferred to the in-leakage air.

The steady state equations were programmed in an Excel spreadsheet. While the number of equations equals the number of variables, direct solution of the equations is very difficult because of the nonlinear nature of the equations, where the radiation terms involve temperatures to the 4^{th} power. Yoshioka used an iterative method to obtain convergence on the cold cap coverage and glass surface temperature. He also assumed a cold cap surface temperature of 100^oC. For this work, a set of 5 nonlinear equations of the form [5] for the glass, cold cap, dome heaters', side wall, and top lid surface radiant heats were written. These equations consisted of temperature terms to the 4^{th} power and linear terms. These were solved by iteration. By comparison to Yosioka's assumption of $100\ ^oC$, the calculated cold cap upper surface temperature ranges from 450^o-477^oC, which is in the film boiling regime for water.

The transient analysis focuses on the melter glass pool, the cold cap, and the steam/air temperature responses. Transient heat balance equations are written for the rate of increase in temperature of the glass pool and the air/vapor mass in the plenum. The cold cap coverage is variable and highly dependent on the difference between the total feed rate and the actual melt rate. Here, a constant cold cap height and porosity is assumed (if changes are slow enough) so that the cold cap expands if the feed rate exceeds the melt rate, and vice-versa. The radiation view factors are functions of the cold cap area and thus vary with time. These result in three simultaneous first order differential equations for the melter glass temperature, the vapor temperature, and the uncovered glass surface area. No time lags are assumed due to radiant heat transfer, boiling, and melting. Additional relations are included for the convective heat flux from the glass pool to the cold cap, the radiant heat flux from the glass surface, the heat flux from the lid heaters, the heat absorbed by the cold cap from the upper plenum. The steam is fully participating in the radiant heat exchange. (In Yosioka's analysis, steam was not included in the radiation exchange.)

BENCHMARKING WITH POWER DATA

To benchmark the lumped parameter model, a calculation was done for two specific Macrobatch 1 conditions provided by the correlations of dome and electrode powers, one at zero feed and the other at 0.7 gpm. The run at zero feed represents a case of the glass surface completely uncovered. The run at 0.7 gpm represents a case of a cold cap area covering 88.8% of the available glass surface area. The calculations use the measured dome heater temperature (950^oC) and the measured vapor temperature (892^oC) corrected for radiant heating.

However, in his comparison with DWPF data, the above correlation under-predicted the DWPF data by as much as 50^oC. This correlation was used in the calculations but was adjusted upwards by 30^0-50^0C, which resulted in better heat balance.

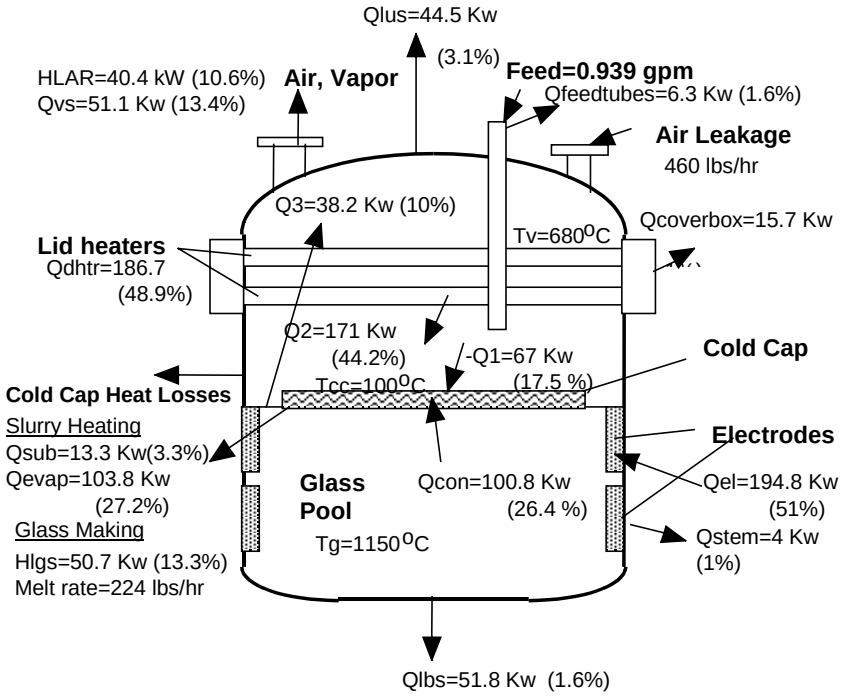

Figure 3 Theoretical Distribution of Power Inputs and Power Consumption for Design Basis Case

An uncontrolled air in-leakage rate of 45.4 Kgs/hr (estimated by DWPF) is also used in addition to the known controlled air in-leakage of 209 Kgs/hr. Also, data for dome heater transformer bus bar cooling are used, as well as natural convection cooling, to add to the heat losses to the lid heater.

In the case of the zero feed run, the total power of 276.4 kW goes into heating the in-leakage air of 254.4 Kgs/hr (47.5 kW), heat loss through the shell of 185.4 kW, and 33.5 kW for miscellaneous losses. The heat loss through the shell was calculated as the difference between the power input and the leakage air loss plus miscellaneous losses.

Design Basis Case – Melt Rate of 224 Lbs/hr

The steady state heat balance is solved using an Excel spreadsheet. Results for the nominal case, considered by Yoshioka (feed rate=0.939 gpm, melt rate of 224 lbs/hr, vapor temperature=680°C, electrode power=194.8 kW, lid heater power=186.7 kW, total air in-leakage flow=460 lbs/hr), are summarized in Figure 19. He assumed a cold cap area coverage of 89% and a glass surface area of 24.7 ft2, taking into account the area taken by the electrodes. The glass melting term includes sensible heating, a silica glass heat of melting (20 cal./gm) and an endothermic reaction heat of -100 cal/gm for the present glass formulation

The component heat losses responsible for slurry heating and evaporation, glass heating, and vapor superheating amount to 218.9 kW or 57.4% of the total power. The total heat losses through the shell (96.3 kW), heating of leakage air (40.4 kW) and miscellaneous losses (26 kW) make up the difference. However, this calculation did not include a number of heat loss sources such as transformer bus bar cooling, radiation into the off-gas outlet flange and other shell penetrations, which significantly increases the total heat loss as evidenced by actual power data.

CONCLUSIONS

A lumped parameter steady and transient thermal analysis model of the DWPF melter has been completed. The steady state analysis has been benchmarked against actual DWPF Melter data. The difference between the design basis predictions and the actual data can be attributed to:

(1) larger heat losses through the melter shell than can be accounted for in the analysis;
(2) scale up effects; and
(3) a larger thermal resistance between the cold cap and the glass melt pool, probably due to a foam layer present with the actual waste, or current nitric acid based feed.

This thermal resistance results in a larger cold cap area for the same feed rate (with less venting) than experienced in the SGM and IDMS runs. Therefore, the design feed rate of 0.939 gpm can not be achieved due to almost complete cold cap coverage at 0.7 gpm for Macrobatch 1 feed and 0.55 gpm for Macrobatch 2 feed.

From these results, it is also concluded that the radiant heat incident on the cold cap is insufficient to completely evaporate the slurry water. Additional heat is required from the glass pool. This heat which passes through the glass/foam layer significantly affects the melt rate.

Other conclusions from the steady state analysis are the following:

- The decrease in electrode power from Macrobatch 1 to Macrobatch 2 and then Macrobatch 3 is consistent with an interface layer buildup on top of the glass of foam or crystalline deposits which reduce heat transfer from the melt pool to the cold cap and hence melt rate.

- A decrease in electrode power for Macrobatch 3 feed under idling conditions is also consistent with an interface layer buildup which reduce heat transfer to the plenum. The lumped model predicts a decreased glass surface temperature

and reduced radiant heat to the plenum, as a result of the reduced measured vapor space temperature.

Recommendations

This lumped parameter model is another step forward after Yosioka's analysis. Understandably, there are still many areas that can be improved upon since large gaps in understanding of many physical processes in the melter still exist. However, the model provides a framework where experimental values or good averages from 3-dimensional CFD analysis of the following parameters can be inserted in place of current assumptions. Improvements in the model should include:

- Convective heat transfer coefficient between cold cap and melt pool for new macrobatches, possibly from bench top slurry melt rate furnace tests,
- Re-evaluation of linearity of cold cap area vs. feed rate, especially at low feed rates, and during transients,
- Values of Hbatch for different macrobatches from bench top experiments,
- Relation between measured and true average dome heater temperatures,
- Average cold cap surface temperature from 3D analysis,
- More accurate determination of the dome heater view factors,
- More accurate determination of glass thermal time constant that includes mixing.

Thus, with input from bench top experiments and iteration with 3-dimensional CFD analysis, a good simple lumped parameter model can be developed for use in evaluating melter performance with new waste macrobatches and also for transient analysis of melter operation.

REFERENCES

[1]. M. Yoshioka to M.D. Boersma, "Prediction of Joule-Heated Glass Melter Operation", NTIS DPST-88-660, 1988.

[2]. Hector G. Guerrero and D.F. Bickford, "Steady and Transient Thermal Analysis of the DWPF Melter Operation", NTIS WSRC-TR-2002-00159, 2002.